Carbohydrate Polymers 111 (2014) 230–235

Contents lists available at ScienceDirect

Carbohydrate Polymers

journal homepage: www.elsevier.com/locate/carbpol

Manganese-containing cellulose nanocomposites: The restrain effect of cellulose treated with NaOH/urea aqueous solutions

Ming-Guo Ma*, Fu Deng, Ke Yao

Beijing Key Laboratory of Lignocellulosic Chemistry, College of Materials Science and Technology, Beijing Forestry University, Beijing 100083, PR China

ARTICLE INFO

Article history:
Received 7 March 2014
Received in revised form 7 April 2014
Accepted 17 April 2014
Available online 26 April 2014

Keywords:
Cellulose
Manganese
Nanocomposites
Restrain effect
Microwave
NaOH/urea

ABSTRACT

In this article, the manganese-containing cellulose nanocomposites were obtained using microcrystalline cellulose and $Mn(CH_3COO)_2{\cdot}4H_2O$ in the NaOH/urea aqueous solutions by a efficient microwave-assisted method. The effects of the heating time and $Mn(CH_3COO)_2{\cdot}4H_2O$ concentration on the cellulose nanocomposites were investigated. It was found that the microcrystalline cellulose pretreated with NaOH/urea aqueous solutions played an important role in the phase, shape, and thermal stability of manganese-containing cellulose nanocomposites. Well-crystalline phases of manganese oxides were not observed in the manganese-containing cellulose nanocomposites. Furthermore, well-crystalline phases of manganese oxides were not also observed by thermal treatment of the manganese-containing cellulose nanocomposites at 600 °C for 3 h. These results could be attributed to the restrain effect of cellulose treated with NaOH/urea aqueous solutions. It was supposed the possible mechanism during the phase transformation of cellulose nanocomposites.

1. Introduction

Cellulose is the most abundant renewable biomass on the earth, which can be converted to high value-added cellulose (nano)composites to meet materials needs (Moon, Martini, Nairn, Simonsen, & Youngblood, 2011). Cellulose (nano)composites held the advantages of cellulose and reinforcement, and had potential applications in optical, catalytic, magnetic, electronic, and biomedical fields (Eichhorn et al., 2010; Siro & Plackett, 2010). In recent years, more attention has been paid to the synthesis of cellulose (nano)composites such as cellulose/Au (Zhang et al., 2010), cellulose/Ag (Sureshkumar, Siswanto, & Lee, 2010), cellulose/CdS (Ke et al., 2009), cellulose/ZnO (Kumar et al., 2011), cellulose/Fe_2O_3 (Liu, Zhang, Zhou, & Wu, 2008), cellulose/TiO_2 (Marques, Trindade, Neto, 2006), cellulose/silica (Cai et al., 2012), cellulose/hydroxyapatite (Grande, Torres, Gomez, & Bano, 2009), and cellulose/$CaCO_3$ (Fu et al., 2013). Many successful strategies including the freezing/freeze-drying method (Svagan, Jensen, Dvinskikh, Furo, & Berglund, 2010), miniemulsion polymerization method (Ben Elmabrouk, Thielemans, Dufresne, & Boufi, 2009), sol–gel process (Siqueira, Mathew, & Oksman, 2011), solvothermal method (Nata, Sureshkumar, & Lee, 2011), hydrothermal method (Ma, Zhu, Li, Jia, & Sun, 2012), microwave-assisted method (Li et al., 2013), ultrasound method (Fu, Yao, Shi, Ma, & Zhao, 2014), and UV-induced modification method (Attia et al., 2013) were employed for the synthesis of cellulose (nano)composites.

The manganese-containing cellulose (nano)composites could be used in water purification and removal of heavy metal ions. There have been a few reports on the fabrication of cellulose/manganese oxide composites or manganese oxide by using cellulose as template (Maliyekkal, Lisha, & Pradeep, 2010; Yin, Gao, Wu, Wang, & Lu, 2010). In situ soft chemical synthesis was used for the fabrication of cellulose-nanoscale-manganese oxide composite with high Pb^{2+} adsorption capacity from aqueous solutions (Maliyekkal et al., 2010). Moreover, the manganese-based nanostructures including Mn_3O_4 octahedrons, MnOOH nanorods, MnO_2 nanowires, and aggregated $MnCO_3$ nanoparticles were prepared through the redox reactions between $KMnO_4$ and sodium carboxymethyl cellulose (Yin et al., 2010). In situ synthesis of manganese dioxide was carried out under ambient conditions on porous cellulose fibers as support with excellent catalytic performance for the oxidative decomposition of formaldehyde (Zhou et al., 2011). An ultrasound-assisted procedure was employed to reduce MnO^{4-} and yield MnO_2 nanoparticles onto natural fique fibers, which could remove up to 98% of the color present in the contaminated water (Chacon-Patino, Blanco-Tirado, Hinestroza, & Combariza, 2013). In the previous study, manganese-containing cellulose nanocomposites were fabricated by an efficient microwave-assisted method, which was used

* Corresponding author. Tel.: +86 10 62336592; fax: +86 10 62336903.
E-mail address: mg_ma@bjfu.edu.cn (M.-G. Ma).

http://dx.doi.org/10.1016/j.carbpol.2014.04.080
0144-8617/

as precursor for the synthesis of Mn_2O_3 by thermal treatment (Li et al., 2013).

It is a promising method of preparing metal oxides by thermal treatment of the cellulose/metal oxides (nano)composites using cellulose as a template. Herein, a facile microwave-assisted method was applied to synthesize the manganese-containing cellulose nanocomposites using microcrystalline cellulose solution and $Mn(CH_3COO)_2{\cdot}4H_2O$. The cellulose solution was prepared by the dissolution of microcrystalline cellulose in the NaOH/urea aqueous solutions. The cellulose pretreatment method had an effect on the manganese-containing cellulose nanocomposites. However, well-crystalline manganese oxides were not obtained before and after the thermal treatment of the manganese-containing cellulose nanocomposites. The restrain effect of cellulose treated with NaOH/urea aqueous solutions was clearly observed during the synthesis and thermal treatment of the manganese-containing cellulose nanocomposites. Research on the restrain effect of cellulose would contribute to the synthesis of metal oxides by thermal treatment of the cellulose/metal oxides (nano)composites using cellulose as a template. Moreover, it provides direct evidence on the interaction between the cellulose and metal ions.

2. Experimental

All chemicals were of analytical grade and used as received without further purification. All experiments were conducted under air atmosphere. The microcrystalline cellulose solution was carried out as previously reported (Jia, Li, Ma, Sun, & Zhu, 2010). In a typical procedure, NaOH (7.00 g) and urea (12.00 g) were dissolved in 81 mL of distilled water to form the NaOH-urea aqueous solution. Then, microcrystalline cellulose (3.24 g, MCC) was added to the NaOH-urea aqueous solution. The above solution was cooled to −12 °C for 12 h. After that, 1.00 g $Mn(CH_3COO)_2{\cdot}4H_2O$ was added into the MCC solution (20 mL) under vigorous magnetic stirring. The solution was heated to 80 °C and kept at this temperature by the microwave heating for 10, 40, and 60 min. The microwave oven used for the samples preparation was purchased from Beijing Xiang-Hu Science and Technology Development Reagent Co., Ltd., which was equipped with the magnetic stirring system and a water-cooled condenser outside the microwave cavity. The resulting precipitate was separated from the solution by centrifugation, washed by distilled water and ethanol several times, and dried at 60 °C for further characterization.

The crystal structure of products was analyzed by an X-ray powder diffraction (XRD) on a Rigaku D/Max 2200-PC diffractometer with Cu Kα radiation (λ = 0.15418 nm) and graphite monochromator at ambient temperature. Scanning electron microscopy (SEM) images were taken with a Hitachi 3400 N scanning electron microscope using an accelerating voltage of 10 kV, which was equipped with an energy dispersive X-ray spectrometer (EDS) operated at 40 kV. Fourier transform infrared (FT-IR) spectroscopy was carried out on an FT-IR spectrophotometer (Nicolet 510) using the KBr disk method. Thermal stability of the cellulose composites was obtained with thermogravimetric analysis (TGA) and differential thermal analysis (DTA) using on a simultaneous thermal analyzer (DTG-60, Shimadzu, Japan) at a heating rate of 10 °C min^{-1} from room temperature to 600 °C.

3. Results and discussion

Based on the simultaneous formation of reinforcement, the precipitation of cellulose, and the fabrication of cellulose nanocomposites, the MCC was pretreated with NaOH/urea aqueous solutions, which could result in a homogeneous distribution of reinforcement in the cellulose matrix. The manganese-containing cellulose nanocomposites were carried out using MCC solution and $Mn(CH_3COO)_2{\cdot}4H_2O$ via a microwave-assisted method at 80 °C. The heating temperature must below 100 °C using water as solvent. In the literature, the Mn_3O_4 polyhedral nanocrystals were obtained using $Mn(CH_3COO)_2{\cdot}4H_2O$ and $(CH_2)_6N_4$ at 80 °C by a microwave-assisted method (Yang, Zhu, Tong, Wang, & Cheng, 2006). Based on the result of literature, the 80 °C was chosen as the heating temperature. The XRD patterns of the typical samples are shown in Fig. 1. The typical peak of cellulose was observed at around $2\theta = 19.1°$ (marked with *, Fig. 1). One can see the decrease peak intensity with increasing heating time, which could be attributed to the interaction between cellulose and reinforcement. Besides the peak of cellulose, the peaks from other impurities were also observed, which did not be assigned to any manganese oxides. In the previous report, the preparation of cellulose-based composites without manganese oxides was reported using MCC, $Mn(CH_3COO)_2{\cdot}4H_2O$, and hexamethylenetetramine in *N*,*N*-dimethylformamide solvent by the microwave-assisted method and Mn_2O_3 materials were obtained by thermal treatment of the cellulose-based composites at 600 °C for 3 h in air (Li et al., 2013).

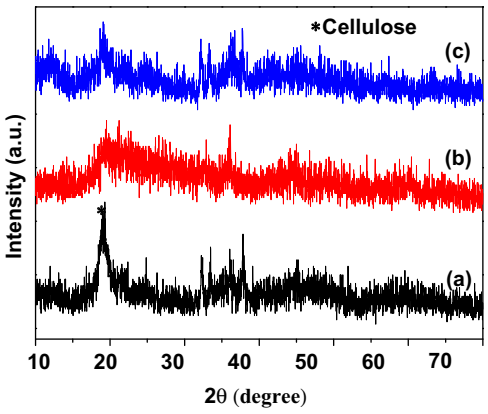

Fig. 1. XRD patterns of the samples prepared at 80 °C for (a) 10 min, (b) 40 min, and (c) 60 min.

In order to confirm the existence of manganese, elemental analysis was conducted for the typical cellulose-based composites. One can observe the elements of C, O, Mn, Cu, and Au in the EDS spectrum (Fig. 2a). The Cu peak is originated from the copper sample holder; meanwhile, the Au peak comes from the preparation procedure of samples prior to examination by SEM. The strong peaks of Mn element were observed, indicating the existence of manganese in the cellulose-based nanocomposites. Fig. 2b–d shows the EDS elemental mapping images of C, O, and Mn, respectively. The even distribution of Mn element further confirmed the fabrication of manganese-containing cellulose nanocomposites. In this experimental system, the reason of absence of well-crystalline manganese oxides is very complex. It was supposed that the MCC treated with NaOH/urea aqueous solutions could affect the synthesis and crystallinity of manganese oxides.

As a typical natural polysaccharide, the functional groups of cellulose are investigated using FT-IR spectra (Fig. 3). The characteristic absorption bands of cellulose at 897 and 1064 cm^{-1} are clearly observed in all the manganese-containing cellulose nanocomposites. The bands at 3449 and 1632 cm^{-1} are the stretching vibration of OH groups and the bending vibrations of the H_2O that absorbed in the cellulose nanocomposites. The peaks at 600 and 514 cm^{-1} are ascribed to the bending modes of Mn—O bonds and cellulose. In comparison with the pure MCC, the manganese-containing cellulose nanocomposites displayed a few difference. For example, the peak intensity at 1453 cm^{-1} increased and the peak intensity at 1064 cm^{-1} decreased. With increasing heating time, the peak at

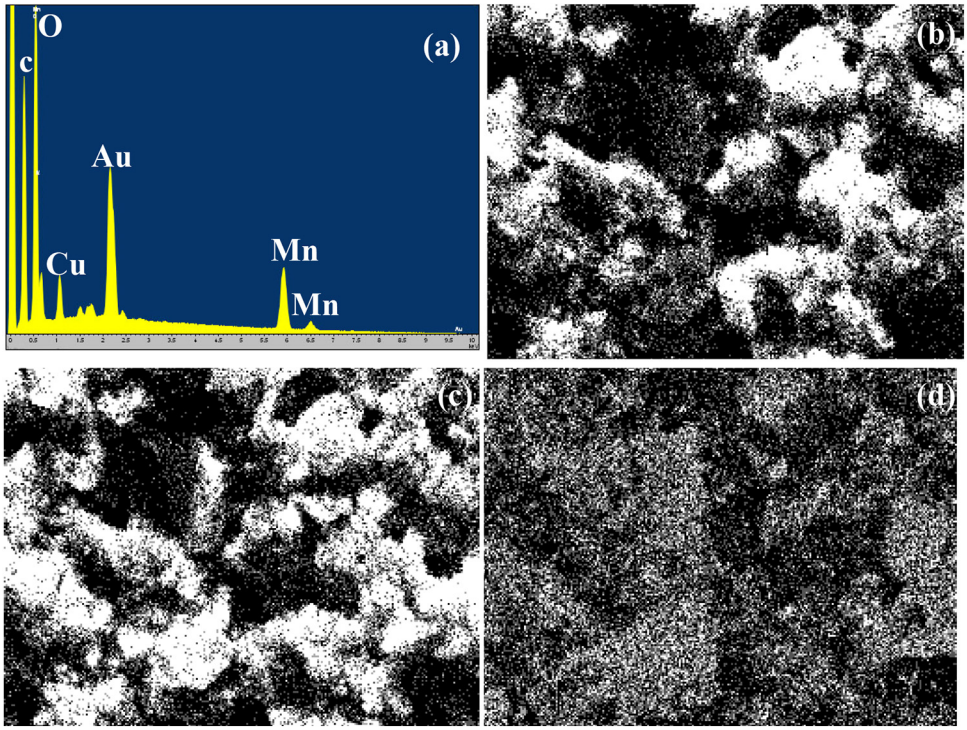

Fig. 2. (a) EDS spectrum and (b–d) the EDS elemental mapping images of the sample prepared by microwave heating at 80 °C for 40 min: (b) C; (c) O; and (d) Mn.

3449 cm^{-1} became broader in the manganese-containing cellulose nanocomposites. In the previous literature, it was reported that the wavenumber movement and became broader of peaks demonstrated a strong interaction between the OH groups of cellulose and reinforcement nanoparticles through hydrogen bonding (Liu et al., 2008). However, it is difficult to obtain the direct evidence of hydrogen bonding in the cellulose-based nanocomposites due to the lack of effective experimental methods and characterization equipments. It is expected that this problem will be solved with the development of measurement technology.

The dispersion of reinforcement in the cellulose matrix is of great importance for potential applications of cellulose nanocomposites. The morphology of the samples was investigated with SEM. It is known that cellulose treated with NaOH/urea displayed an irregular flake-like shape. When the heating time was 10 min, irregular cellulose flakes were observed (Fig. 4a). Magnification images of the sample showed aggregated nanosheets (Fig. 4b and c),

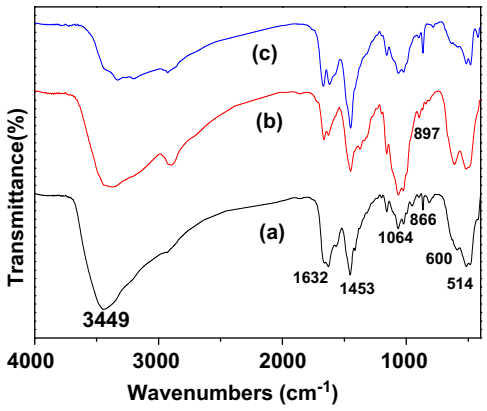

Fig. 3. FT-IR spectra of the manganese-containing cellulose nanocomposites prepared at 80 °C for (a) 10 min, (b) 40 min, and (c) 60 min.

which should belong to the manganese-containing reinforcement based on the literature and experimental results. Increased the heating time to 40 min, the nanosheets grow on the cellulose substrate and the size of nanosheets dramatically decreased (Fig. 4d–f). When the heating time was 60 min, the nanosheet bundles were observed at the surface of cellulose (Fig. 4g–i). These results demonstrated that the heating time had an effect on the shape and size of the manganese-containing cellulose nanocomposites. In the previous literature, a few manganese-containing particles were dispersed in the cellulose matrix (Li et al., 2013). In this article, the manganese- containing reinforcement with nanosheet-like shape was obtained. Obviously, the pretreatment method and solvents had a great influence on the shape of manganese-containing reinforcement.

The influence of $Mn(CH_3COO)_2{\cdot}4H_2O$ concentration on the manganese-containing cellulose nanocomposites was also investigated, as shown in Fig. 5. Decreased $Mn(CH_3COO)_2{\cdot}4H_2O$ concentration from 1.00 g to 0.50 g and 0.25 g, the cellulose with irregular shape was still clearly observed and no nanosheets were obtained, demonstrating that the $Mn(CH_3COO)_2{\cdot}4H_2O$ concentration had an effect on the shape of manganese-containing reinforcement.

In general, the metal oxides were obtained by thermal treatment of the metal oxides-containing cellulose nanocomposites. The thermal treatment temperature was decided based on the results of TGA and DTA. As shown in Fig. 6, the total weight losses of the manganese-containing cellulose nanocomposites were ~52.5% (10 min), ~62.7% (40 min), and ~58.4% (60 min) from room temperature to 600 °C in the TGA curves, respectively. Weight losses were observed during the total thermal treatment procedure, which could not be divided into different stages. This result was completely different from the previous reports (Li et al., 2013; Ma et al., 2012). MCC has an obvious weight loss in the region 250–380 °C; meanwhile, the cellulose treated with NaOH/urea solution also displayed a weight loss in the region 250–380 °C (Li, Jia, Zhu, Ma, & Sun, 2010). Moreover, the cellulose nanocomposites showed two

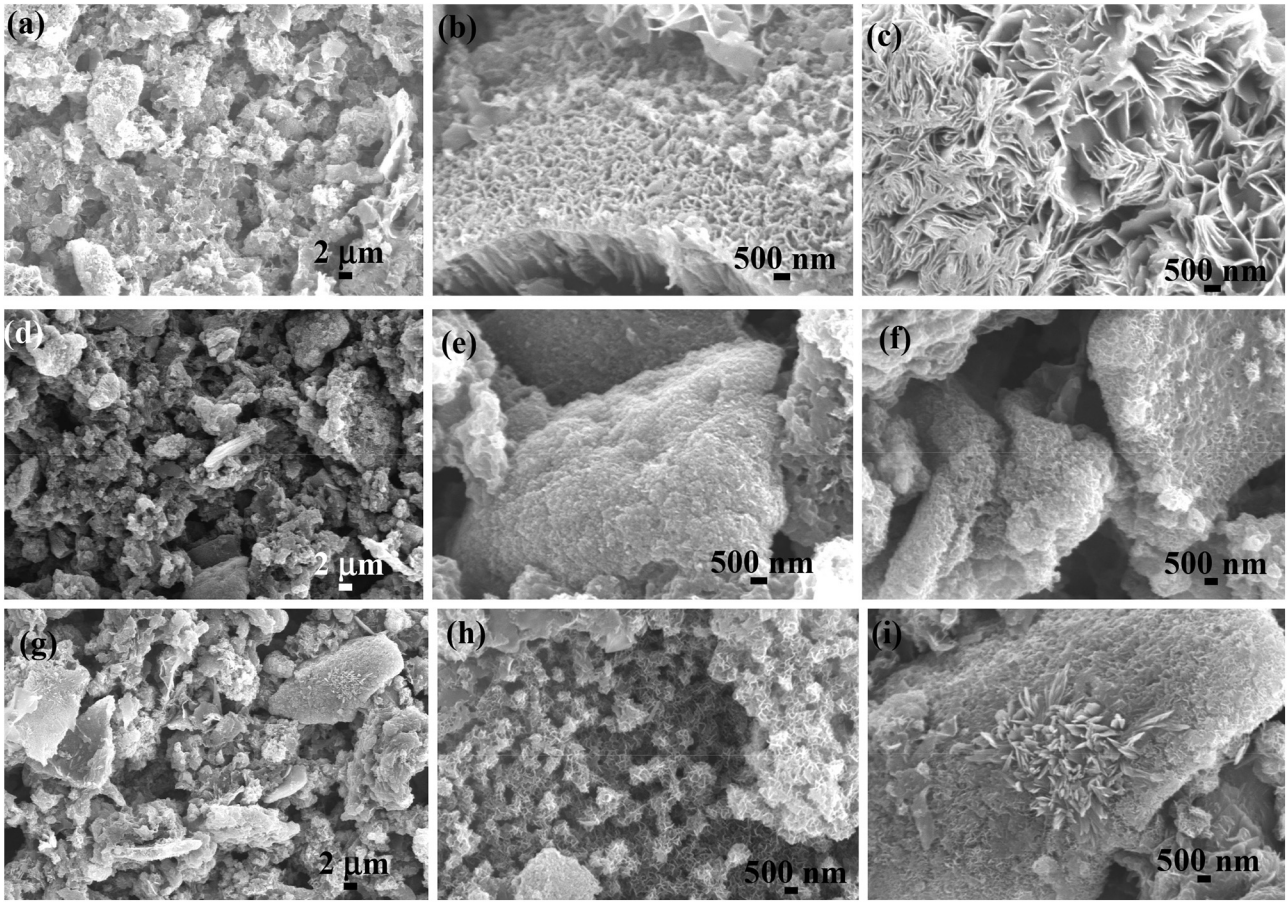

Fig. 4. SEM images of the manganese-containing cellulose nanocomposites prepared at 80 °C for (a–c) 10 min, (d–f) 40 min, and (g–i) 60 min.

weight losses stages assigning to the thermal degradation and complete decomposition of cellulose in the composites (Li et al., 2013). From the DTA curves, no obvious exothermic peaks were also observed. The XRD, SEM, and FT-IR results confirmed the existence of cellulose. It was supposed that the different thermal stability of the manganese-containing cellulose nanocomposites could be attributed to the interaction between cellulose and manganese-containing particles by the addition of manganese to the cellulose. Of course, there are still the lack of indirect and enough evidence to support this suppose.

In view of the results of TGA and DTA, the 600 °C was chosen as the thermal treatment temperature using the manganese-containing cellulose nanocomposites as precursor. The original purpose was to obtain the manganese oxides by calcination of cellulose. However, XRD pattern of the sample, which was obtained by calcination of the manganese-containing cellulose nanocomposites at 600 °C for 3 h, indicated the synthesis of amorphous manganese-containing materials (Fig. 7a). This result was different from previous report (Li et al., 2013). The shape of calcination sample displayed some irregular shape and sheet-like shapes with several hundred nanometers (Fig. 7b). Magnification image of the sample clearly displayed sheet-like shapes (Fig. 7c).

Next we discuss the possible mechanism of the synthesis and phase transformation of manganese-containing cellulose nanocomposites. In this article, the manganese-containing cellulose nanocomposites were obtained using MCC solution and $Mn(CH_3COO)_2{\cdot}4H_2O$ by a microwave-assisted method. The MCC solution was prepared by the dissolution of MCC in the NaOH/urea aqueous solutions. In comparison with the previous reported results, some interesting phenomena were observed. Based on the

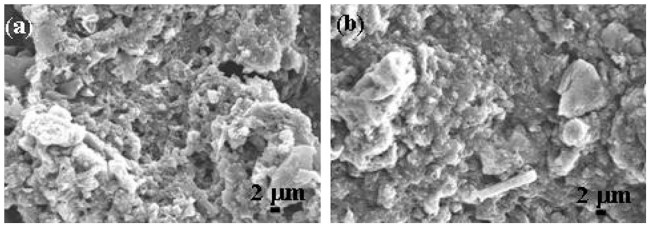

Fig. 5. SEM images of the samples prepared by microwave heating at 80 °C for 40 min using different $Mn(CH_3COO)_2{\cdot}4H_2O$ concentrations: (a) 0.50 g and (b) 0.25 g.

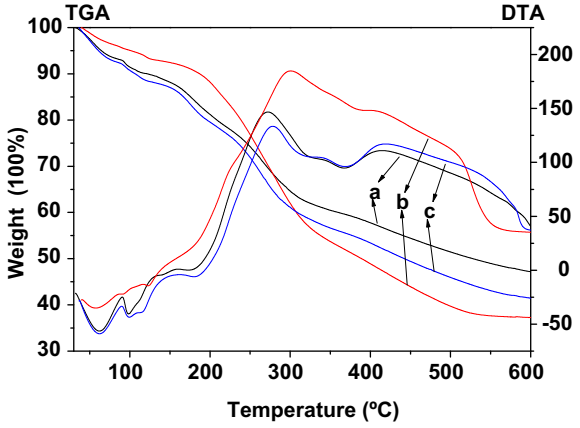

Fig. 6. TGA and DTA curves of the manganese-containing cellulose nanocomposites prepared at 80 °C for (a) 10 min, (b) 40 min, and (c) 60 min.

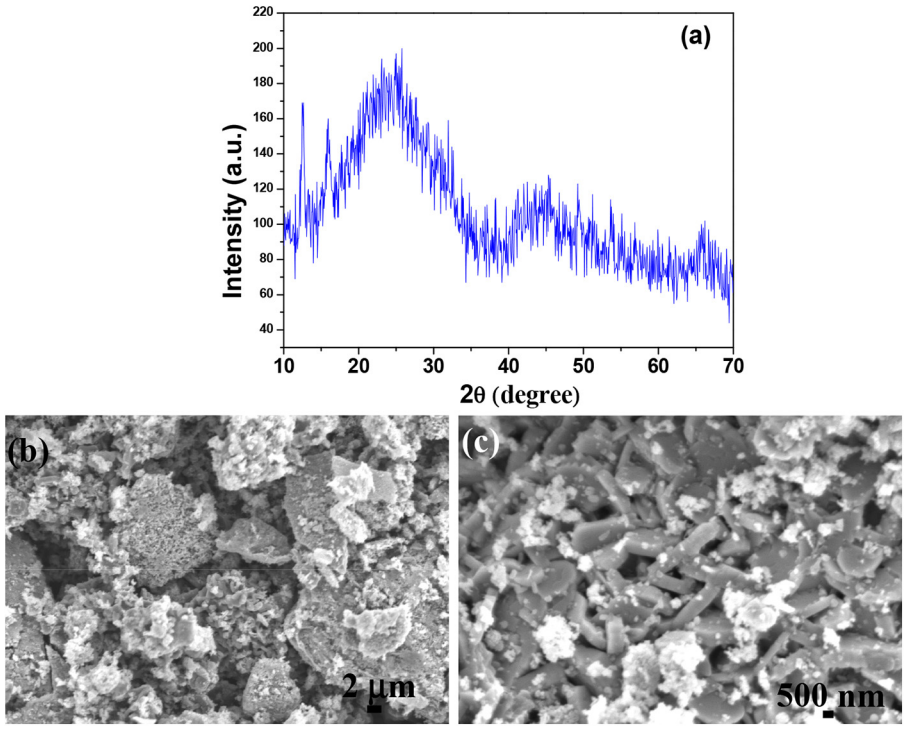

Fig. 7. XRD pattern (a) and SEM images (b and c) of the sample by thermal decomposition of the manganese-containing cellulose nanocomposites at 600 °C for 3 h.

previous knowledge and experimental results, one can observe that no well-crystalline manganese oxides were obtained during the synthesis and phase transformation of manganese-containing cellulose nanocomposites. EDS analysis confirmed the existence of manganese in the cellulose-based nanocomposites. In the previous literature, it was reported that the phase transformation of α-FeOOH to α-Fe_2O_3 was restrained in the cellulose/iron oxide nanocomposites by a hydrothermal method (Ma et al., 2012) and the phase transformation from $Cu(OH)_2$ to CuO was restrained in the cellulose/$Cu(OH)_2$/CuO hybrids during the sonochemistry process (Fu et al., 2014). Moreover, as mentioned above, it was reported that cellulose-based composites without manganese oxides were obtained by the microwave-assisted method (Li et al., 2013). Therefore, it was supposed that the absence of well-crystalline manganese oxides could be attributed to the restrain effect of cellulose pretreated NaOH/urea aqueous solutions. It is known that cellulose has the intra- and inter-molecular hydrogen bonds. Mn^{2+} has strong coordination ability. It is suggested that the Mn^{2+} bound with the OH-groups along the polymer chains, leading to the enrichment of Mn^{2+} on the surface of cellulose. Besides, the synthesis of manganese-containing cellulose nanocomposites was based on the simultaneous formation of manganese-containing particles and precipitation of the cellulose, which resulted in a homogeneous distribution of manganese-containing particles in the cellulose matrix. During the thermal treatment procedure, the MCC decomposed and residual was manganese-containing materials. It was supposed that the presence of cellulose pretreated NaOH/urea aqueous solutions inhibited the crystallinity of manganese oxides, inducing the fabrication of amorphous manganese-containing materials. During the preparation process of cellulose/metal oxides composites, the restrain effect of cellulose was not always observed. Therefore, the detained mechanism still needs to be further explored in the near future. Since the basic formation mechanisms are still poorly understood, there is still much room to improve the syntheses of metal oxides in the cellulose nanocomposites. More attentions should be paid to the research of manganese-containing cellulose nanocomposites.

4. Conclusions

In summary, the microwave-assisted route was reported for the synthesis of the manganese-containing cellulose nanocomposites. Well-crystalline manganese oxides were not obtained before and after thermal treatment of the manganese-containing cellulose nanocomposites due to the restrain effect of cellulose pretreated NaOH/urea aqueous solutions. These results demonstrated that the MCC pretreated with NaOH/urea solution had an important influence on the phase, shape, and thermal stability of the manganese-containing cellulose nanocomposites. Research on the restrain effect of cellulose would be helpful for understanding the synthesis of metal oxides by thermal treatment of the cellulose/metal oxides (nano)composites using cellulose as a template.

Acknowledgments

Financial support from the Fundamental Research Funds for the Central Universities (No. JC2013-3), Beijing Nova Program (Z121103002512030), and the Program for New Century Excellent Talents in University (NCET-11-0586) is gratefully acknowledged.

References

Attia, M. F., Azib, T., Salmi, Z., Singh, A., Decorse, P., Battaglini, N., et al. (2013). One-step UV-induced modification of cellulose fabrics by polypyrrole/silver nanocomposite films. *Journal of Colloid and Interface Science*, *393*, 130–137.

Ben Elmabrouk, A., Thielemans, W., Dufresne, A., & Boufi, S. (2009). Preparation of poly(styrene-co-hexylacrylate)/cellulose whiskers nanocomposites via miniemulsion polymerization. *Journal of Applied Polymer Science*, *114*, 2946–2955.

Cai, J., Liu, S. L., Feng, J., Kimura, S., Wada, M., Kuga, S., et al. (2012). Cellulose-silica nanocomposite aerogels by in situ formation of silica in cellulose gel. *Angewandte Chemie-International Edition*, *51*, 2076–2079.

Chacon-Patino, M. L., Blanco-Tirado, C., Hinestroza, J. P., & Combariza, M. Y. (2013). Biocomposite of nanostructured MnO_2 and fique fibers for efficient dye degradation. *Green Chemistry*, *15*, 2920–2928.

Eichhorn, S. J., Dufresne, A., Aranguren, M., Marcovich, N. E., Capadona, J. R., Rowan, S. J., et al. (2010). Review: Current international research into cellulose nanofibres and nanocomposites. *Journal Materials Science*, *45*, 1–33.

Fu, L. H., Dong, Y. Y., Ma, M. G., Yue, W., Sun, S. L., & Sun, R. C. (2013). Why to synthesize vaterite polymorph of calcium carbonate on the cellulose matrix via sonochemistry process? *Ultrasonics Sonochemistry*, *20*, 1188–1193.

Fu, L. H., Yao, K., Shi, C. M., Ma, M. G., & Zhao, J. J. (2014). Ultrasonic-assisted synthesis of cellulose/$Cu(OH)_2$/CuO hybrids and its thermal transformation to CuO and Cu/C. *Science of Advanced Materials*, *6*, 1117–1125.

Grande, C. J., Torres, F. G., Gomez, C. M., & Bano, M. C. (2009). Nanocomposites of bacterial cellulose/hydroxyapatite for biomedical applications. *Acta Biomaterialia*, *5*, 1605–1615.

Jia, N., Li, S. M., Ma, M. G., Sun, R. C., & Zhu, J. F. (2010). Hydrothermal synthesis and characterization of cellulose-carbonated hydroxyapatite composites in NaOH-urea aqueous solution. *Science of Advanced Materials*, *2*, 210–214.

Ke, D. N., Liu, S. L., Dai, K., Zhou, J. P., Zhang, L., & Peng, T. Y. (2009). CdS/regenerated cellulose nanocomposite films for highly efficient photocatalytic H-2 Production under visible light irradiation. *Journal of Physical Chemistry C*, *113*, 16021–16026.

Kumar, A., Gullapalli, H., Balakrishnan, K., Botello-Mendez, A., Vajtai, R., Terrones, M., et al. (2011). Flexible ZnO-cellulose nanocomposite for multisource energy conversion. *Small*, *7*, 2173–2178.

Li, S. M., Jia, N., Zhu, J. F., Ma, M. G., & Sun, R. C. (2010). Synthesis of cellulose-calcium silicate nanocomposites in ethanol/water mixed solvents and their characterization. *Carbohydrate Polymers*, *80*, 270–275.

Li, S. M., Wang, Y. L., Ma, M. G., Zhu, J. F., Sun, R. C., & Xu, F. (2013). Microwave-assisted method for the synthesis of cellulose-based composites and their thermal transformation to Mn_2O_3. *Industrial Crops and Products*, *43*, 751–756.

Liu, S. L., Zhang, L., Zhou, J. P., & Wu, R. X. (2008). Structure and properties of cellulose/Fe_2O_3 nanocomposite fibers spun via an effective pathway. *Journal of Physical Chemistry C*, *112*, 4538–4544.

Ma, M. G., Zhu, J. F., Li, S. M., Jia, N., & Sun, R. C. (2012). Nanocomposites of cellulose/iron oxide: Influence of synthesis conditions on their morphological behavior and thermal stability. *Materials Science and Engineering C*, *32*, 1511–1517.

Maliyekkal, S. M., Lisha, K. P., & Pradeep, T. (2010). A novel cellulose-manganese oxide hybrid material by in situ soft chemical synthesis and its application for the removal of Pb(II) from water. *Journal of Hazardous Materials*, *181*, 986–995.

Marques, P. A. A. P., Trindade, T., & Neto, C. P. (2006). Titanium dioxide/cellulose nanocomposites prepared by a controlled hydrolysis method. *Composites Science and Technology*, *66*, 1038–1044.

Moon, R. J., Martini, A., Nairn, J., Simonsen, J., & Youngblood, J. (2011). Cellulose nanomaterials review: Structure properties and nanocomposites. *Chemical Society Reviews*, *40*, 3941–3994.

Nata, I. F., Sureshkumar, M., & Lee, C. K. (2011). One-pot preparation of amine-rich magnetite/bacterial cellulose nanocomposite and its application for arsenate removal. *RSC Advances*, *1*, 625–631.

Siqueira, G., Mathew, A. P., & Oksman, K. (2011). Processing of cellulose nanowhiskers/cellulose acetate butyrate nanocomposites using sol–gel process to facilitate dispersion. *Composites Science and Technology*, *71*, 1886–1892.

Siro, I., & Plackett, D. (2010). Microfibrillated cellulose and new nanocomposite materials: A review. *Cellulose*, *17*, 459–494.

Sureshkumar, M., Siswanto, D. Y., & Lee, C. K. (2010). Magnetic antimicrobial nanocomposite based on bacterial cellulose and silver nanoparticles. *Journal of Materials Chemistry*, *20*, 6948–6955.

Svagan, A. J., Jensen, P., Dvinskikh, S. V., Furo, I., & Berglund, L. A. (2010). Towards tailored hierarchical structures in cellulose nanocomposite biofoams prepared by freezing/freeze-drying. *Journal of Materials Chemistry*, *20*, 6646–6654.

Yang, L. X., Zhu, Y. J., Tong, H., Wang, W. W., & Cheng, G. F. (2006). Low temperature synthesis of Mn_3O_4 polyhedral nanocrystals and magnetic study. *Journal of Solid State Chemistry*, *179*, 1225–1229.

Yin, J. Z., Gao, F., Wu, Y. F., Wang, J. J., & Lu, Q. Y. (2010). Synthesis of Mn_3O_4 octahedrons and other manganese-based nanostructures through a simple and green route. *CrystEngComm*, *12*, 3401–3403.

Zhang, T. J., Wang, W., Zhang, D. Y., Zhang, X. X., Ma, Y. R., Zhou, Y. L., et al. (2010). Biotemplated synthesis of gold nanoparticle-bacteria cellulose nanofiber nanocomposites and their application in biosensing. *Advanced Functional Materials*, *20*, 1152–1160.

Zhou, L., He, J. H., Zhang, J., He, Z. C., Hu, Y. C., Zhang, C. B., et al. (2011). Facile in-situ synthesis of manganese dioxide nanosheets on cellulose fibers and their application in oxidative decomposition of formaldehyde. *Journal of Physical Chemistry C*, *115*, 16873–16878.